Journal of Chromatography A, 1218 (2011) 5456–5469

Contents lists available at ScienceDirect

Journal of Chromatography A

journal homepage: www.elsevier.com/locate/chroma

Modifying conventional high-performance liquid chromatography systems to achieve fast separations with Fused-Core columns: A case study

A.J. Alexander[a,*], T.J. Waeghe[b], K.W. Himes[a], F.P. Tomasella[a], T.F. Hooker[a]

[a] Analytical Research and Development, Bristol Myers Squibb Company, 1 Squibb Drive, New Brunswick, NJ 08903, USA
[b] MAC-MOD Analytical, Inc.,103 Commons Court, Chadds Ford, PA 19317, USA

ARTICLE INFO

Article history:
Received 15 July 2010
Received in revised form 4 June 2011
Accepted 7 June 2011
Available online 17 June 2011

Keywords:
Fast LC
Fused-Core®
Extra-column dispersion
Extra-column band broadening
Extra-column volume

ABSTRACT

The theoretical increase in performance from the use of high efficiency columns with conventional HPLC equipment is generally not observed due to the design limitations of such equipment, particularly with respect to extra-column dispersion (ECD). This study examines the impact of ECD from a Waters Alliance 2695 system on the performance of 2.7 μm HALO® C_{18} Fused-Core superficially porous particle columns of various dimensions. The Alliance system was re-configured in different ways to reduce extra-column volume (ECV) and the ECD determined in each case as a function of flow rate up to a maximum of 2 mL/min. The results obtained showed a progressive decrease in ECD as the ECV was reduced, irrespective of the flow rate employed. However, this decrease in ECD was less than theoretically expected for the lower ECV configurations. The inability to reduce the actual extra-column dispersion further was attributed to additional dispersion associated with the design/volume of the auto-injector. This was confirmed by making sample injections with a low dispersion manual injection valve, instead of auto-injection, for the two lowest ECV configurations studied. In each case, the measured and predicted ECD values were in good agreement. The auto-injector module is an integral part of the Alliance 2695 instrument and cannot be easily modified. However, even with autosampler injection, for a 3 mm ID × 100 mm Fused-Core® column approximately 70% of the maximum plate count (~84% of the resolution or more) could still be obtained in isocratic separations for solutes with $k \geq \sim 4.5$ when using the lowest ECV configuration. This study also highlights some of the problems inherent in trying to measure accurately the true extra-column dispersion of a chromatographic system and compares the results obtained to those theoretically predicted. Using this same lowest volume instrument configuration, two real-world pharmaceutical methods were scaled to separations that are ~3–3.5-fold faster, while still maintaining comparable data quality (resolution and signal-to-noise ratios).

1. Introduction

Prior to the recent commercialization of ultra high pressure liquid chromatography (UHPLC), the column format of choice for the LC profiling of impurities in pharmaceutical products had evolved to be 4.6 mm ID × 150 mm packed with either 3 μm, or 3.5 μm, particles [1,2]. However, since the introduction of UHPLC, increasing emphasis has been placed on scaling existing methods to utilize narrower bore columns packed with smaller (sub-2 μm) particles [3–5]. With reduced column diameters and corresponding lower flow rates, the added benefit of reducing solvent consumption has been realized. Another key technological advancement has been the recent commercialization of sub-3 μm superficially porous particles, which were commercialized first by Advanced Materials Technology in 2007 (2.7 μm HALO® Fused-Core® particles [6] and more recently by Phenomenex (both 2.6 μm and 1.7 μm Kinetex™ particles) [7]. These particles provide a significant improvement in column efficiency (≥200,000 plates/m) but generate only 40–50% of the backpressure (2.6 and 2.7 μm particles only) produced by sub-2 μm columns [8–11]. This pressure advantage allows fast LC methods to be developed with these columns utilizing conventional pressure (<400 bar) LC equipment [12–14]. However, due to the design limitations of these systems, particularly with respect to extra-column dispersion (ECD) and detector limitations, the full theoretical performance of these columns is generally not realized [15,16]. In order to achieve such performance, particularly in isocratic mode, critical components and settings of the chromatographic system and software have to be optimized [16]. In particular, the extra-column volume (ECV) has to be reduced to within an acceptable level [8,14–17]. The contributions to ECD arise primarily from two major sources. The first one is largely volumetric in nature and derives from the injection volume, detector volume and volume of the interconnecting tubing in the sample flow path. The second stems from time-related events, such

* Corresponding author. Tel.: +1 732 227 6737.
E-mail address: Anthony.Alexander@bms.com (A.J. Alexander).

0021-9673/$ – see front matter © 2011 Elsevier B.V. All rights reserved.
doi:10.1016/j.chroma.2011.06.026

as the detector/data system-sampling rate and the detector time constant. These ECD contributions have been recognized since the early days of chromatographic instrument development and extensive mathematical treatments have been presented in the literature [18–22].

From a practical aspect, ECD on older modular systems can be significantly reduced by reducing the ECV contribution from each of the critical modules (injector and detector volumes) and interconnecting tubing volume [9,16]. This modification can often be simply achieved by appropriate substitution of suitable low volume chromatographic parts from the original instrument vendor, or from third-party suppliers. However, in doing so, it is important to note that ECV is just one contribution to ECD. The actual internal design of the various chromatographic components themselves (UV flow cell, injection valve, connectors, column inlet fittings, etc.) can also significantly affect ECD, independent of their volume contribution [15,22]. Thus, one cannot necessarily assume that the other contributions to ECD are negligible compared to ECV alone. Nevertheless, significant reductions in ECD (and corresponding improvements in performance) have been achieved by simply reducing the ECV of the HPLC system. For example, a conventionally configured Agilent 1100 quaternary system has ~35 μL of extra-column volume (w_{ec}), whereas, after appropriate reduction in ECV, this can be reduced to ~11 μL [16]. A similar study found that the ECD of a standard Agilent 1100 binary system could be reduced from 41.5 μL^2 to 13.7 μL^2 by minimization of the needle seat capillary volume, the connector tubing volumes and the volume of the detector flow cell [15]. For comparison, a very low dispersion LC system (Waters Acquity UPLC) has between 9 μL and 12 μL of extra-column band broadening (calculated from reported σ^2_{ec} values (ECD) of 5 μL^2 [23] and 8.5 μL^2 [15] and a reported σ_{ec} value of 2.8 μL respectively) [24].

On older, less versatile semi-modular systems, reducing the ECV may not be such a simple undertaking. In the case of the Alliance 2695 Separations Module from Waters Corporation, the auto-injector does not use a multi-port rotary injection valve with a fixed loop (as is the case with the Agilent 1100 HPLC), but instead uses a proprietary Seal-Pack injection system [25]. This module is an integral part of the chromatograph and cannot be easily modified. Although the UV detector is modular (usually supplied as either a Waters model 2487 dual wavelength UV detector, or a Waters model 2996 photodiode array detector [PDA]), the options for flow cell replacement are limited. These factors combine to make the modification of this instrument for fast LC less than straightforward. With regard to minimizing the time-related contribution to ECD, the modification of older detector modules is generally not practical. Thus, one is limited to using the minimum time constant and maximum sampling rate settings available, which will generally impose a performance penalty [26]. The question is just how severe this will be for the separation conditions employed (see Section 2).

In this work, we present the results of a systematic study (using model analytes) to determine the factors that limit the performance of the Alliance 2695 for fast LC separations, and we offer guidance regarding what chromatographic efficiencies can be expected for various levels of modification. Finally, using a modified instrument, we present real world examples of existing pharmaceutical impurity separations (with early eluting components) that have been converted to significantly faster methods without loss in resolution.

2. Theory

2.1. Extra-column dispersion (ECD)

In order to obtain the highest possible efficiency from a column, it is necessary to reduce all sources of dispersion from the liquid chromatographic system. The band (or peak) dispersion from the chromatographic column itself can be conveniently expressed by:

$$\sigma^2_{col} = \frac{V_r^2}{N_{col}} = \frac{V_{col}^2(1+k)^2}{N_{col}} \quad (1)$$

where V_r is the retention volume of the solute eluted under isocratic conditions, V_{col} is the column void volume, k is the retention factor, N_{col} is the theoretical column efficiency and σ_{col} is the standard deviation of the peak in volume units [27]. Thus, if N_{col} is relatively large (highly efficient column) and V_{col} is relatively small (as is the case for fast LC with small column dimensions and low total porosity), then column-related dispersion (particularly for analytes with small k values) will be correspondingly smaller and the relative impact of the fixed amount of instrument-related extra-column dispersion will be significantly greater.

Extra-column dispersion (σ^2_{ec}) is normally expressed in terms of four main sources of chromatographic dispersion, which are assumed to be independent, and therefore, additive [21]:

$$\sigma^2_{ec} = \sigma^2_{inj} + \sigma^2_{conn} + \sigma^2_{det} + \sigma^2_{elec} \quad (2)$$

where σ^2_{inj}, σ^2_{conn}, σ^2_{det}, and σ^2_{elec} are variances due to the injector, the connecting tubing and unions, the detector flow cell, and signal processing electronics, respectively.

As a general rule, in a well-designed chromatographic system, the extra-column dispersion should contribute no more than a total 10% loss in efficiency (~5% loss in resolution), that is, $\sigma^2_{ec} \leq 0.1\sigma^2_{obs}$ where σ^2_{obs} is the actual observed peak variance [20,21]. This parameter (σ^2_{obs}), is comprised not only of the dispersion from the chromatographic process itself (σ^2_{col}), but also of the aforementioned extra-column dispersion occurring elsewhere in the HPLC system [20], That is:

$$\sigma^2_{obs} = \sigma^2_{col} + \sigma^2_{ec} = \frac{V_r^2}{N_{obs}}$$

where N_{obs} is the observed column efficiency. The observed column-related and extra-column-related peak widths (in volume units) are also related similarly, that is:

$$w^2_{obs} = w^2_{col} + w^2_{ec}.$$

This means that $\sigma_{ec} \leq 0.32\sigma_{obs}$, and therefore w_{ec}, the extra-column volume, should be no greater than about one third of the peak volume (w_{obs}) of the narrowest peak of interest in the chromatogram.

The various sources of dispersion identified in Eq. (2) can be quantified and the following general expression for σ^2_{ec} (in units of μL^2) obtained [27]:

$$\sigma^2_{ec} = \left(\frac{K_{inj} \cdot V_{inj}^2}{12}\right) + \frac{\pi r^4 \cdot l \cdot F}{24 D_m} + \left(\frac{K_{cell} \cdot V_{cell}^2}{12}\right) + \tau^2 \cdot F^2 \quad (3)$$

where K_{inj} and K_{cell} are constants (generally between 1 and 3 [28]) that are characteristic of the injection profile and the geometry of the UV cell, respectively; F is the flow rate in units of μL/s; and D_m is the analyte diffusion coefficient in the mobile phase in units of mm^2/s. The lowest possible contribution from the injection process occurs when $K_{inj} = 1$, which corresponds to a perfectly rectangular sample plug [28]. Clearly, in order to reduce σ^2_{ec}, the injection volume V_{inj} (μL), the radius r (mm) and length l (mm) of the connecting tubing, the flow-cell volume V_{cell} (μL), and the detector time constant τ (s) must all be minimized.

The second contribution term in Eq. (3) (corresponding to σ^2_{conn} in Eq. (2)) is the Taylor–Aris equation. However, this expression only strictly applies at lower flow rates (≤~0.2 mL/min) and overestimates the dispersion at higher flow rates, as recently demonstrated by Fountain et al. [see [24] and references therein]. They proposed the expression $\sigma^2_{conn} = (\pi r^2 \cdot l)^2/(3 + 24\pi \cdot l \cdot D_m/F)$

to better describe the dispersion as a function of flow rate, although this equation still overestimates, but to a lesser extent, the dispersion at higher flow rates. Interestingly, above a flow rate of ~0.3 mL/min, the actual measured dispersion in straight 50-cm lengths of tubing, with internal diameters ranging from 0.0025″ to 0.010″, was found to be essentially constant (for a given diameter) with increasing flow rate up to 2 mL/min (Fig. 3, Ref. [24]). If this modification to the way σ^2_{conn} is calculated is taken into account, the effective extra-column dispersion can be estimated as:

$$\sigma^2_{ec} = \left(\frac{K_{inj} \cdot V^2_{inj}}{12}\right) + \frac{(\pi r^2 \cdot l)^2}{3 + 24\pi \cdot l \cdot D_m/F'} + \left(\frac{K_{cell} \cdot V^2_{cell}}{12}\right) + \tau^2 \cdot F^2 \quad (4)$$

where F' is the actual flow rate when working in the range ≤ 5.0 μL/s ($\leq$0.3 mL/min), but is a constant, with a value of 5, when the flow rate exceeds a value of 5.0 μL/s.

2.2. Calculation of maximum acceptable extra-column volume (w_{ec})

A useful expression can be derived to calculate the amount of extra-column volume (w_{ec}) that will allow one to achieve a desired fractional amount of the maximum theoretical column efficiency (N_{obs}/N_{col}) for a given column:

$$w_{ec} = 4 \times \left[\frac{V^2_{col}(k+1)^2}{N_{col}} \times \frac{1 - (N_{obs}/N_{col})}{(N_{obs}/N_{col})}\right]^{1/2} \quad (5)$$

This parameter (w_{ec}), recorded in units of μL, where $w_{ec} = 4\sigma_{ec}$, is also commonly referred to as the instrumental bandwidth [29], and is related to the extra-column dispersion by the expression $\sigma^2_{ec} = [w_{ec}/4]^2$. For example, in order to maintain at least 90% of the resolving power ($N_{obs}/N_{col} = 0.81$) of a 3.0 mm ID × 100 mm Fused-Core column, with $V_{col} = 356$ μL, $N_{col} = 22{,}000$ and $k = 2$, w_{ec} must not exceed 14 μL. This amount of tolerable extra-column volume is 40% lower than the maximum allowed (23 μL) for a conventional 3-μm particle size column of the same dimensions ($V_{col} = 459$ μL, $N_{col} = 13{,}300$). The column void volume, V_{col}, was calculated from the total porosity value of 0.506 published by Gritti et al. [30] for Fused-Core columns, whereas a value of 0.65 was assumed for the conventional column.

2.3. Calculation of maximum acceptable detector cell volume

Within the general guidance of limiting $\sigma^2_{ec} \leq 0.1\sigma^2_{obs}$, the variance associated with the detector in a well-designed chromatographic system is generally limited to 5% of the column variance, that is, $\sigma^2_{det} \leq 0.05\sigma^2_{col}$ [21]. This stipulation can be combined with Eq. (1) and the equation for σ^2_{det}, obtained from Eq. (3), to yield the following equation:

$$\frac{K_{cell} \times V^2_{cell}}{12} = 0.05\sigma^2_{col} = \frac{0.05V^2_{col}(1+k)^2}{N_{col}}$$

If K_{cell} is set to its typical value of 3, this equation can be solved for V_{cell} to yield:

$$V_{cell} \leq \left[\frac{0.2 \times V^2_{col}(1+k)^2}{N_{col}}\right]^{1/2} \quad (6)$$

If we consider a 3.0 mm ID × 100 mm Fused-Core column for an analyte with $k = 2$, $V_{col} = 356$ μL, $N_{col} = 22{,}000$, then the flow cell volume must be $\leq$3.2 μL.

2.4. Calculation of maximum acceptable detector response time

With respect to the limits placed on the time constant of the detector, it has been shown [19] that, if the fractional decrease in theoretical efficiency is limited to be less than θ^2, then the time constant τ should be smaller than:

$$\tau \leq \frac{\theta \times t_r}{(N_{col})^{1/2}} \quad (7)$$

where t_r is the retention time of the peak in seconds. The full response time (actually 10–90% of the full response) of the detector takes 2.197 time constants and is referred to as the response time (τ_R) [31]. As the % band spreading due to the time constant is equal to $100 \times \theta^2$, and as $t_r = t_0 \times (1 + k)$ with $t_0 = V_{col}/F$ (t_0 is the retention time of an unretained peak), then Eq. (7) can be solved for (maximum allowable) response time (τ_R):

$$\tau_R \cong 2.2\tau \leq 2.2 \times \left[\left(\frac{\%\,\text{band spreading}}{100}\right)^{1/2} \times (1+k) \times \frac{V_{col}/F}{(N_{col})^{1/2}}\right] \quad (8)$$

where V_{col} is in mL and F is in mL/s for τ_R to be in s.

If we consider a 3.0 mm ID × 100 mm Fused-Core column with an analyte eluting at $k = 2$ with a flow rate of 0.95 mL/min, $V_{col} = 0.356$ mL, $N_{col} = 22{,}000$ and $F = 0.0158$ mL/s, then the time constant $\tau \leq 0.1$ s and the response time $\tau_R \leq 0.22$ s (if the maximum % spreading is to be limited to 5%). Note, if the more conservative requirement of limiting the maximum % band spreading to 1% is employed, in order to allow greater individual contributions to the overall variance from σ^2_{inj} and σ^2_{det} in Eq. (4), then the time constant $\tau \leq 0.05$ s, and response time $\tau_R \leq 0.1$ s.

2.5. Calculation of minimum detector sampling rate

With respect to the limits placed on the sampling rate of the detector, at least 20 data points should be collected across the narrowest peak of interest to define the peak profile accurately [32]. As the observed standard deviation of the peak in time units is given by $\sigma_{obs} = t_r/(N_{obs})^{1/2}$, then the observed peak width in time units can be expressed as:

$$w_{obs} = 4\sigma_{obs} = 4 \times \frac{t_0(1+k)}{(N_{obs})^{1/2}} = 4 \times \frac{V_{col}}{F} \times \frac{1+k}{(N_{obs})^{1/2}}$$

Hence:

$$\text{Detector sampling rate} \geq \frac{20}{w_{obs}} \geq \frac{5 \times F \times (N_{obs})^{1/2}}{V_{col} \times (1+k)} \quad (9)$$

If we consider a 3.0 mm ID × 100 mm Fused-Core column with $N_{col} = 22{,}000$ and $F = 0.95$ mL/min, and incorporate a maximum 10% overall loss in efficiency due to extra-column band broadening (i.e. $N_{obs} = 0.9N_{col}$), then the required detector sampling rates should be $\geq$15.7 Hz for a peak eluting at $k = 1$ and $\geq$10.5 Hz for $k = 2$.

3. Experimental

3.1. Chemicals and reagents

All solvents were HPLC grade. Acetonitrile was purchased from EMD Chemicals (Gibbstown, NJ, USA) and water was purified in-house using a Milli-Q UV Plus purification system (Millipore Corp, Billerica, MA, USA). Uracil, anisole, nitrobenzene, benzonitrile, 1-chloro-4-nitrobenzene and ethylbenzene were purchased from Sigma–Aldrich (Milwaukee, WI, USA). Benzyl alcohol and toluene were purchased from J.T. Baker (Phillipsburg, NJ, USA). Naphtho[2,3-a]pyrene was purchased from TCI America (Portland, OR, USA). Proprietary pharmaceutical drug substances

BMS-708163 {(R)-2-(4-chloro-N-(2-fluoro-4-(1,2,4-oxadiazol-3-yl)benzyl)phenylsulfonamido)-5,5,5-trifluoropentanamide [33]} and BMS-727740 {N-(4-fluoro-2-(5-methyl-1H-1,2,4-triazol-1-yl)benzyl)-3-hydroxy-9,9-dimethyl-4-oxo-4,6,7,9-tetrahydropyrimido[2,1-c][1,4]oxazine-2-carboxamide [34]} were synthesized in-house.

3.2. Instrumentation

An Alliance 2695 Separations Module, equipped with either a model 2487 dual wavelength UV detector or a model 2996 PDA (all from Waters Instruments, Inc., Milford, MA), was used for this study. In our hands, the "standard configuration" of this instrument had 253 mm of pre-column tubing (from auto-injector valve outlet to column inlet) and 605 mm of post column tubing (from column outlet to flow cell inlet). In each case, the tubing was 1/16th in. OD × 0.009 in. ID stainless steel. Note that the pre-column tubing supplied by Waters (part # WAT270979) is 30 in. long (762 mm), and is generally cut back on installation to a length appropriate to reach the column oven module mounted on the right hand side of the instrument. Also, note that the original oven heat exchanger tubing was removed and not employed in this study. The standard 2487 UV detector was fitted with an analytical flow cell of 10 μL internal volume and 10 mm path length (part # WAS081140). The standard 2996 PDA was fitted with an analytical flow cell of 8 μL internal volume and 10 mm path length (part # WAT057919). The internal diameter of the input tubing was 0.009 in. ID for both analytical flow cells.

Alternative micro-flow cells were purchased from Waters for each detector. The only change that was made to these cells was that the column connection tubing was cut back to a length of 605 mm in each case. The 2487 micro-bore cell (part # WAT081159) has an internal volume of 2.6 μL and a path length of 3 mm. The PDA micro-flow cell (part # WAT057462) has an internal volume of 1.7 μL and a path length of 6 mm. The internal diameter of the input tubing was 0.005 in. ID for both micro-bore cells. In the case of the 2487 cell design, the input tubing is connected directly to the cell via a brazed joint and, hence, cannot be replaced. The 2996 cell design does not suffer from this limitation as the inlet tubing can be removed completely from the cell via a nut and ferrule connection. The only other modification undertaken was to replace the standard 100 μL injection syringe on the auto-injector module with the micro syringe option (25 μL syringe, Waters part # WAT077343).

The standard Alliance 2695 System described above was modified in three different ways, the details of which are summarized in Table 1 together with an estimate of the ECV for each configuration, which was obtained by summing the known volumes in the sample flow path.

In order to assess the contribution of σ^2_{inj} from the auto-injector module in configuration 3, a low dispersion manual injection valve (Rheodyne Model 8125, IDEX Corporation, Rohnert Park, CA) was installed in the flow path just before the column. Specifically, the outlet tubing from the auto-injector valve (existing 260 mm × 0.005 in. ID stainless steel) was connected directly to the manual injection valve inlet, and the valve outlet was connected to the column inlet using a 100 mm length of 0.005 in. ID PEEK tubing. This resulted in the auto-injector being effectively removed from the *sample flow path*, although the mobile phase was still being delivered *through* the auto-injector module. The manual valve was fitted with a 5 μL stainless steel loop, which was filled by means of a 10 μL gas tight glass manual syringe. The injection volume was 2 μL and the internal volume of the valve was ~0.5 μL (value determined by manufacturer). The minimum ECV, from the manual injection valve to the detector, was estimated to be 14.5 μL for configuration 3 and 7.5 μL for alternate configuration 3. In each case, these values were obtained by summing the known volumes in the sample flow path. For the experiments carried out with this valve, termed manual valve injection, the Alliance 2695 was programmed to initiate each chromatographic run by making a blank injection of mobile phase and to record the UV detector output. Coincident with the start of the blank injection and data collection, a partial-loop injection of the actual sample was made using the manual injection valve. The valve was then left in the inject position during the remainder of each chromatographic run.

3.3. Chromatographic conditions

3.3.1. Extra-column dispersion measurements

Extra-column dispersion measurements for each configuration were obtained by replacing the column with a zero dead volume connector [35–37]. Measurements were obtained by both autosampler and manual valve injections using uracil, anisole and naphtho[2,3-a]pyrene as test probes. Uracil was selected as it is commonly used as an unretained marker and naphtho[2,3-a]pyrene was selected as it has been previously used by other researchers [14,15] and therefore can be used for comparative purposes. Anisole was also included as it was the compound employed in the current study for the van Deemter measurements. The mobile phases were pre-mixed 50:50 water/acetonitrile for uracil and anisole and pure acetonitrile for naphtho[2,3-a]pyrene. Measurements were obtained over a range of flow rates (0.2–2 mL/min in increments of 0.2 mL/min) at a temperature of 30 °C. Sample concentrations were adjusted to give approximately equal UV responses within the target range of 50 mAU. The injection volume was 1 μL and the sample diluent was the same as that of the respective mobile phase composition. UV detection was performed at a wavelength of 254 nm for uracil and anisole and 294 nm for naphtho[2,3-a]pyrene. All chromatograms obtained with the 2487 dual wavelength UV detector were acquired with the minimum time constant of 0.1 s and the maximum single channel sampling rate of 10 Hz. Data were acquired with the 2996 PDA at the maximum sampling rate of 10 Hz and with a zero filter setting. To provide sufficient backpressure at low flow rates a 250-psi backpressure regulator was connected to the output of the detector. Instrument control, data acquisition and data manipulation were performed using Empower software, feature release 2 (Waters, Inc.). Peak variances (σ^2_{obs} values in μL^2 units) for each analyte were obtained from the expression $\sigma^2_{obs} = [w_{obs}/5]^2$, where w_{obs} is the peak width at 4.4% of peak height (5σ peak width) recorded in volume units (μL). The 5σ peak width was chosen to minimize the impact of the peak tailing that is typically observed for injections without a column present, as was done by McCalley [14]. The data were measured in triplicate, with a relative standard deviation ($n-1$) of less than 1% for all flow rates. The peak variances at each flow rate were also obtained by calculating the second moment (M_2) of each peak. This was accomplished by exporting the Empower raw data files (as AIA files) so they could be handled by Agilent ChemStation software (Rev. B.01.03), which can produce extended reports showing moment analysis of peaks. The diffusion coefficients ($D_{A,B} \times 10^{-5}$ cm^2/s) of anisole and naphtho[2,3-a]pyrene, as estimated from the Wilke–Chang equation, were 1.32 in ACN–water (50:50, v/v) at 30 °C and 1.29 in pure ACN at 30 °C [38].

3.3.2. Column efficiency measurements with autosampler injection

Isocratic separations were carried out using (1) a 3.0 mm ID × 100 mm, (2) a 4.6 mm ID × 50 mm, or (3) a 2.1 mm ID × 50 mm 2.7 μm HALO® C_{18} Fused-Core® columns (MAC-MOD Analytical, Chadds Ford, PA, USA) operated at optimum linear velocities of

Table 1
Modifications to Alliance 2695 system (with autosampler). N/A: not applicable.

Instrument description	Configuration change	Pre-column tubing (mm)	Post-column tubing (mm)	Detector model	Flow cell vol. (μL)	Estimated ECV[a] (μL)
Config. 1	N/A	253 (1/16 × 0.009 in.)	605 (1/16 × 0.009 in.)	2487	10	45
Config. 2	Micro-bore cell with 0.005 in. ID tubing	253 (1/16 × 0.009 in.)	605 (1/16 × 0.005 in.)	2487	2.6	21
Config. 3	Micro-bore cell, 0.005 in. ID tubing throughout	260 (1/16 × 0.005 in.)	605 (1/16 × 0.005 in.)	2487	2.6	14
Alternate config. 3	Micro-bore cell with 0.004 in. ID tubing, 0.005 in. ID pre-column tubing	260 (1/16 × 0.005 in.)	300 (1/16 × 0.004 in.)	2996	1.7	8

[a] The extra-column volume (ECV) for each configuration was estimated by summing the known volumes in the sample flow path, that is, the tubing volume and flow cell volume.

3 mm/s and at a temperature of 30 °C. The mobile phase was 50:50 water/acetonitrile and sample injections were performed with both the autosampler and by use of a manual injection valve. The sample consisted of a mixture of analytes (substituted benzenes): uracil (void marker), benzyl alcohol, benzonitrile, nitrobenzene, anisole, 1-chloro-4-nitrobenzene and toluene at concentrations adjusted to give approximately equal UV responses within the target range of 10–50 mAU. The injection volume was 2 μL. The sample solvent strength was approximately equal to that of the mobile phase (~50% ACN) or slightly lower. UV detection was performed at a wavelength of 254 nm. All chromatograms obtained with the 2487 dual wavelength UV detector were acquired with the minimum time constant of 0.1 s and the maximum single channel sampling rate of 10 Hz. Data were acquired with the 2996 PDA at the maximum sampling rate of 10 Hz and with a zero filter setting. Instrument control, data acquisition and data manipulation were performed using Empower software, feature release 2 (Waters). The N_{obs} values for each analyte were obtained by measurement of the peak width at 4.4% of peak height (5σ peak width) in each case to be consistent with the no-column measurements. Uracil was used as the void time (t_0) marker. The diffusion coefficients ($D_{A,B} \times 10^{-5}$ cm^2/s) of benzyl alcohol, benzonitrile, nitrobenzene, anisole, 1-chloro-4-nitrobenzene and toluene, as estimated from the Wilke–Chang equation, were 1.35, 1.37, 1.36, 1.32, 1.23 and 1.33 respectively in ACN–water (50:50, v/v) at 30 °C [38].

3.3.3. van Deemter measurements with autosampler injection

Separations were performed isocratically over the flow rate range 0.1–0.95 mL/min using a 3.0 mm ID × 100 mm 2.7 μm HALO® C_{18} Fused-Core® column operated at a temperature of 30 °C. The mobile phase was 50:50 water/acetonitrile and the injection volume was 2 μL. All measurements were acquired at 254 nm using the Waters 2487 UV detector with a time constant of 0.1 s and a sampling rate of 10 Hz. The sample consisted of a mixture of anisole and ethylbenzene at concentrations adjusted to give approximately equal UV responses within the target range of 10–50 mAU at 254 nm. The linear velocity employed, the so-called chromatographic velocity (u), was calculated from the expression $u = L/t_0$ where L is the length of the column and t_0 is the retention time of the void volume marker (uracil) at each specific flow rate. The N_{obs} values used to calculate the respective HETP values were obtained by measurement of the peak width at 13.4% of peak height (4σ peak width) in each case.

3.3.4. Gradient impurity profiling of BMS-708163 and BMS-727740

A 3.0 mm ID × 100 mm 2.7 μm HALO® C_{18} Fused-Core® column, operated at a temperature of 40 °C and at a flow rate of 0.9 mL/min, was used for each separation. All measurements were carried out using a Waters 2487 UV detector, with a time constant of 0.1 s and a single-channel sampling rate of 10 Hz. A common injection volume of 3 μL was employed. BMS-708163, at a concentration of 0.15 mg/mL in 50:50 (v/v) water/acetonitrile, was chromatographed with detection at 244 nm. The mobile phases were water (phase A) and acetonitrile (phase B). The gradient program was as follows: 0.0–7.0 min: 42%B, 10.5 min: 100%B, 10.6 min: 42%B, and 13.0 min stop. BMS-727740, at a concentration of 0.2 mg/mL in 90:10 (v/v) water/acetonitrile, was chromatographed with detection at 232 nm. The mobile phase constituents were 10 mM potassium phosphate adjusted to pH 2.1 with phosphoric acid (phase A) and acetonitrile (phase B). The gradient program employed was as follows: 0.0–7.0 min: 22%B, 10.5 min: 70%B, 10.6 min: 22%B, and 13.0 min stop. N_{obs} values for the various sample components were obtained by measurement of the respective peak widths at 13.4% of peak height (4σ peak width).

4. Results and discussion

4.1. Theoretical column performance as a function of extra-column dispersion

Useful guidance on the performance that can be expected from columns when operated in isocratic mode using conventional chromatographic equipment can be obtained from Eqs. (5)–(7) and (9). In Table 2, the impact of various amounts of extra-column volume is shown on the performance of columns suitable for the impurity profiling of pharmaceutical products, which includes conventional 3.5 μm totally porous columns and 2.7 μm Fused-Core columns in several diameters and lengths (3.0 and 4.6 mm IDs, 100 and 150 mm lengths).

A calculated maximum extra-column volume w_{ec} value of 46 μL (which corresponds to an extra-column band spreading, or variance, of 132 μL^2) was used as a comparison point for the standard Alliance 2695 system. This value is in good agreement with our estimated ECV value for the un-modified configuration (see Table 1). Extra-column volume w_{ec} values reported in the literature for the Waters Alliance 2695 system range from 29 μL [25] to 31 μL [39], but these values are for non-standard systems, i.e., some form of optimization had been carried out, such as reducing the post-column tubing size from 0.009 in. to 0.005 in. ID [40].

As can be seen in Table 2, operation with 4.6 × 150 conventional columns, for which the Alliance 2695 system was primarily designed, presents no problem, as the minimum k value is 1 and the maximum t_c and minimum DR values are all within range of the Waters 2487 UV detector (see Section 3.3.1). Alternatively, if a 3 × 150 conventional column is employed to reduce solvent consumption, then the resulting minimum k value is significantly higher (3.6 versus 1). In this situation, w_{ec} must be reduced to ~20 μL to regain the original k value. If a more efficient 4.6 × 100 Fused-Core® column is employed with a standard Alliance, an increase in minimum capacity factor (now 3.6 versus 1) must be accepted, if the desired gain in efficiency is to be realized, although

Table 2
Instrumental parameters required for the impurity profiling of pharmaceutical products using both conventional and Fused-Core columns.

Column type	Column dimensions	Flow rate [a] (mL/min)	Est. V_{col} [b] (mL)	Est. N_{col}	Max. w_{ec} (μL)	Min. k value	Max. t_c [c] (s)	Min. DR (Hz)	Max. flow cell vol. (μL)
Type B, 3.5 μm	4.6 × 150	1	1.570	17,100	46.0	1.0	0.14	4	11
Type B, 3.5 μm	3 × 150	0.5	0.668	17,100	46.0	3.6	0.28	2	11
Type B, 3.5 μm	3 × 150	0.5	0.668	17,100	19.8	1.0	0.12	4	5
HALO, 2.7 μm	4.6 × 100	1.5	0.841	26,400	46.0	3.6	0.09	5	11
HALO, 2.7 μm	4.6 × 100	1.5	0.841	26,400	20.1	1.0	0.04	12	5
HALO, 2.7 μm	3 × 100	0.64	0.358	24,700	46.0	9.4	0.22	2.2	11
HALO, 2.7 μm	3 × 100	0.64	0.358	24,700	8.8	1.0	0.04	11.7	2

Minimum detector sampling rate (DR) was calculated assuming a minimum of 20 data points across the peak. w_{ec} values were calculated on the basis of maintaining over 90% of the resolving power of the column, that is $N_{obs}/N_{col} = 0.81$. N_{col} values were calculated assuming a reduced plate count of 1.4 and 1.5 for 4.6 and 3.0 mm ID Fused-Core columns, respectively, and a reduced plate count of 2.5 for the type B column. The maximum flow cell volumes were calculated assuming $K_{cell} = 3$. The standard flow cell available for the Alliance 2695 has a volume of 10 μL; alternately available micro-flow cells have volumes of 2.6 μL and 1.7 μL (see Section 3).

[a] Calculated from an optimum linear velocity of 3 mm/s for Fused-Core and 1.8 mm/s for totally porous type B silica columns.

[b] Calculated assuming a total column porosity of 0.506 for Fused-Core and 0.65 for totally porous, type B columns.

[c] Calculated assuming a % broadening value of 1%.

both values of t_c and DR are still acceptable. However, to reduce the minimum k value to 1, then w_{ec} must be reduced from to 46 μL to 20 μL. If, on the other hand, a 3 × 100 Fused-Core® column is employed to gain both an improved efficiency and to reduce solvent consumption, an even greater increase in minimum capacity factor (9.4 versus 1) must be tolerated, unless w_{ec} is reduced from 46 μL to 8.8 μL. Nevertheless, even if it were possible to reduce w_{ec} to this level, then the required minimum t_c, maximum DR and maximum flow-cell volume values would be out of the range of the Waters 2487 UV detector (0.04 s, 11.7 Hz, and 2 μL, respectively).

In this study, a 3 mm × 100 mm Fused-Core® column was selected for further study, in conjunction with reducing w_{ec} to the lowest practical value, as this diameter provides the benefit of reduced solvent consumption while maintaining the required sample loading capacity required for impurity profiling. A column length of 100 mm is the shortest that can be employed for this purpose, as shorter columns do not provide the necessary separation efficiency, while longer columns usually generate too much backpressure for Alliance systems (>5000 psi) under gradient operation. It can be seen that, based on the estimated ECV, only configuration 3 (and alternate configuration 3) are likely to meet the calculated minimum requirements for efficient operation of this size of column if $k \geq 2$, that is, estimated ECV ≤ 14 μL, and a flow cell volume contribution of ≤3 μL (see Table 1).

4.2. Determination of extra-column dispersion using the "no-column method"

The experimentally measured ECD values for the configurations listed in Table 1, obtained as a function of flow rate, are shown in Fig. 1(a)–(d) using both uracil and naphtho[2,3-a]pyrene as test probes. For each configuration, both the second moment (M_2) and 5σ-derived dispersions are shown for each analyte. The rationale for doing this is as follows. Although exact numerical integration of the peak (statistical moments) is considered the most accurate method, it can overestimate the variance due to errors arising from the integration limits, the baseline drift and noise [41,42]. In addition, it is more difficult to relate this value to the plate number of a peak obtained when the column is present (N_{obs}), because column efficiencies are usually calculated from the actual peak widths measured at specific points on the peak (either at 1/2 height, or 4σ, or 5σ).

Considering the results obtained with auto-injection first, the following general observations can be made. Firstly, the 5-sigma derived peak variances are systematically smaller than the M_2 calculated variances, which is to be expected, and both exhibit the same general trend with respect to flow rate. Secondly, for configuration 1, the ECD values are essentially constant with increasing flow rate above ~0.4 mL/min for both test probes and for both computational methods. Thirdly, for all other configurations, ECD increases with increasing flow rate above a certain threshold value, with the order of threshold value increase being configuration 2 > configuration 3 > alternate configuration 3. This threshold flow rate is analyte-dependent, and is ~1 mL/min for uracil and ~0.8 mL/min for naphtho[2,3-a]pyrene. As well as being characteristic of the instrument configuration, such peak variance dispersions are also dependent on the nature of the analyte, the viscosity of the mobile phase [14,15], and on the temperature employed [24]. In this case, the results obtained with naphtho[2,3-a]pyrene are systematically smaller than those obtained with uracil, but only for configuration 1. In the case of configurations 2 and 3, ECD values for naphtho[2,3-a]pyrene are greater than those for uracil at flow rates above ~1 mL/min. Interestingly, this trend does not hold for alternate configuration 3, where again the trend in ECD values is comparable for both test probes. These results confirm the importance, as articulated by McCalley [14], of assessing the impact of extra-column dispersion under the same conditions used for the subsequent analysis.

Comparison of the results, irrespective of the test probe used, clearly shows a progressive decrease in ECD from configuration 1 to alternate configuration 3, which is consistent with the concomitant decrease in ECV (see Table 1). The most significant decrease in ECD is obtained when changing from configuration 1 to configuration 2, as would be expected, because this change involves the largest reduction in ECV, which mainly is due to the decrease in the flow cell volume. In comparison, the change from configuration 2 to configuration 3 involves only a reduction in the pre-column tubing volume, and this is consistent in a smaller decrease in the measured ECD values. Interestingly, the change from configuration 3 to alternate configuration 3, which would be expected to have a significant impact on ECV (see Table 1), resulted in only a marginal decrease in ECD across the flow rate range. However, it must be noted that with lower ECVs and higher flow rates, the ability to record accurately the very narrow peak profiles is limited by the maximum detector data sampling rate and time constant. The data sampling rate should always be faster than the mobile phase refresh rate in the respective flow cells, and factors as high as 2.5-fold higher have been used to ensure adequate data were taken for the no-column experiments [42]. In this study, due to the limited data sampling rate of 10 Hz, we are close to the minimum 1:1 data sampling rate/mobile phase refresh rate ratio for flow rates >1.4 mL/min for configurations 2 and 3 and for flow rates >1 mL/min for alternate configuration 3. The restrictions imposed by the limited time constant are even more severe. According to Sternberg [18], peak fidelities of 0.99, 0.95 and 0.90 require the time constant to be 1/16th, 1/7th and 1/5th of the peak width at half-height, respectively. With a minimum time constant of 0.1 s,

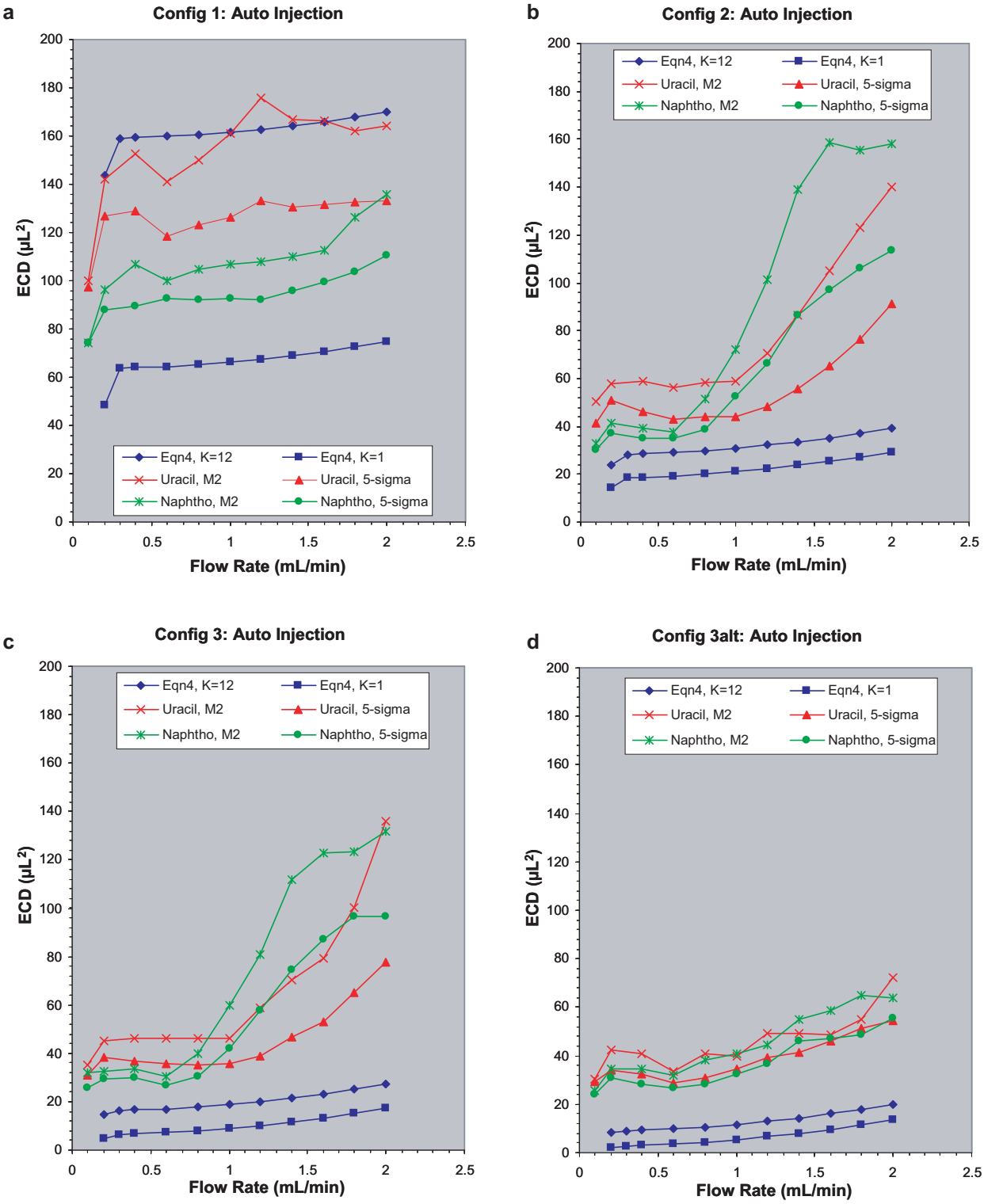

Fig. 1. (a–d) Measured ECD (σ^2_{ec}) values as a function of flow rate for configurations shown in Table 1 with auto-injection: (a) configuration 1, (b) configuration 2, (c) configuration 3 and (d) alternate configuration 3. The test analytes were uracil with mobile phase 50/50 (v/v) acetonitrile:water and naphtho[2,3-a]pyrene with mobile phase 100% acetonitrile in each case. For each analyte, both the second moment (M_2) and 5σ-derived dispersions are shown. The theoretical peak variances as a function of flow rate, obtained from Eq. (4) are also plotted with the following limits for the constants: $1 < K_{inj} < 12$ and $1 < K_{cell} < 12$. Abbreviations for data legend: naphtho, naphtho[2,3-a]pyrene.

95% fidelity of the no-column peak profile (0.95) cannot be achieved for flow rates >1.2 mL/min for configurations 2 and 3 and for flow rates >0.8 mL/min for alternate configuration 3. However, the 90% fidelity condition (0.90) was satisfied for all flow rates employed for configurations 2 and 3 and for flow rates up to 1.4 mL/min for alternate configuration 3.

In plots 1(a)–1(d) the theoretical peak variances as a function of flow rate, obtained from Eq. (4) are also plotted with the following limits for the constants: $1 < K_{inj} < 12$ and $1 < K_{cell} < 12$. It is important to note that, in Eq. (4), F' is the actual flow rate at values $\leq$0.3 mL/min and capped at this value when the flow rate exceeds 0.3 mL/min, that is, $F' = 0.3$ mL/min for *all* flow rate conditions above

Table 3
Measured ECV (w_{ec} at 5σ) and calculated extra-column dispersion [$[\sigma^2_{ec} = ((w_{ec}/5)^2)]$] values for different instrument configurations, as measured by no-column method using uracil and naphtho[1,4]pyrene as test probes. The measured values for w_{ec} are average values calculated from triplicate analyses. The values obtained for naphtho[1,4]pyrene are shown in square brackets. Injection volume 1 μL, mobile phases: 50:50 (v/v) acetonitrile/water for uracil and 100% acetonitrile for naphtho[1,4]pyrene. See Table 1 for descriptions of each configuration and estimated ECV values.

Flow rate (mL/min)	Instrument configuration	Measured ECV (w_{ec}, μL)	Calculated band spreading ECD (σ^2_{ec}, μL^2)	ECV difference measured minus estimated (μL)
1.0	Config. 1	56 [48]	126 [93]	11 [3]
	Config. 2	33 [36]	44 [53]	12 [15]
	Config. 3	30 [33]	36 [42]	16 [19]
	Alt. config. 3	29 [28]	34 [32]	21 [20]
2.0	Config. 1	58 [53]	133 [111]	13 [8]
	Config. 2	48 [53]	91 [114]	27 [32]
	Config. 3	44 [49]	78 [96]	30 [35]
	Alt. config. 3	37 [37]	54 [56]	29 [29]

0.3 mL/min. Theoretically, the lowest possible contribution from the injection process occurs when $K_{inj} = 1$, which corresponds to a perfectly rectangular sample plug [21]. Whereas, the limit of $K_{inj} = 12$ corresponds to the situation where the injector produces an exponential injector profile [21]. The physical meaning of the limits for K_{cell} is analogous, with the detector sensing volume generating either a rectangular peak dispersion profile ($K_{cell} = 1$), or an exponential (mixing) profile ($K_{cell} = 12$). In the real world, the dispersion profiles produced by both the injector and the detector are some combination of these two limiting cases, and, as such, these constants are typically assigned values of 3 for well designed systems [28]. In the case of configuration 1, Eq. (4) reasonably predicts the experimentally observed dispersion, however the limits between $K_{inj} = 1$ and $K_{inj} = 12$ are wide (~100 μL^2) due to the contribution from σ^2_{det}, which results from the relatively large volume of the analytical flow cell employed (10 μL). For configurations 2–3alt, the theoretical limits are narrower, due primarily to the smaller flow cells (see Table 1). For these configurations, Eq. (4) also reasonably predicts the trend of the experimentally observed dispersion up to a flow rate of ~1 mL/min. However, in each case, the experimental values are ~20–30 μL^2 higher than expected, depending on the nature of the test probe employed. That is, there appears to be a fixed amount of additional dispersion within the system that becomes apparent only when the total dispersion is significantly reduced. Above 1 mL/min, the observed dispersion progressively increases at a rate that is significantly higher than predicted by Eq. (4). This could partly be explained by the increased demands put on the detection system to define accurately the progressively narrower peak profiles (see above discussion). The M_2 calculation is more sensitive to changes in peak shape caused by inadequate definition of the profile and the calculated variance is biased high under these circumstances. Thus, if distortion of the peak profile occurs, a greater divergence between the 5-sigma and M_2 data would be expected, which is indeed the case at the higher flow rates studied (particularly for configurations 2 and 3). Consequently, at higher flow rates, where the data are clearly limited by the detector time constant and data collection rate, these plots are more aptly described as "instrument fingerprints", rather than reflecting the actual (real) levels of extra-column dispersion present.

The measured w_{ec} values and derived ECD values, obtained with both uracil and naphtho[2,3-a]pyrene at flow rates of 1 mL/min and 2 mL/min, are shown for each configuration in Table 3. The 1-mL/min flow rate is of particular interest as it is approximately the maximum flow rate that can be attained with a 3.0 mm ID × 100 mm Fused-Core® column using ~90% of the available backpressure limit of the Alliance 2695 system. [The Alliance 2695 is rated for a maximum backpressure of 5000 psi, and at an initial gradient condition of 42% acetonitrile with a column temperature of 40 °C, the backpressure obtained was 4600 psi].

In an initial analysis, the experimentally derived w_{ec} results were compared against the estimated ECV values (from Table 1) for the respective configurations. The results, also tabulated in Table 3, show a progressively widening disparity between these two sets of data as the actual ECV of the system was reduced. That is, at a flow rate of 1 mL/min there appeared to be, in the worst case, an equivalent of up to ~20 μL of extra-column volume that could not be accounted for (Table 3, column 4). At a flow rate of 2 mL/min this discrepancy further increased to ~30–35 μL. It is important to recognize that the absolute values of these differences are dependent on how the actual extra-column peak variance is determined [41,42]. In this case, σ^2_{ec} was calculated using σ obtained from the 5σ peak width (see Section 2.1). This was done to minimize the impact of the inherent tailing (which is characteristic of no-column peak profiles) on the calculated variance values and to be consistent with the work of McCalley [14]. If data from the second moment calculations had been used, these differences would have had slightly greater absolute values, as illustrated in Fig. 1(a)–(d), but the same trend would have prevailed. Fountain et al. [24], who have previously published extra-column band broadening data for the Alliance 2695 system, measured the peak widths at 4σ. A σ^2_{ec} value of ~42 μL^2 was obtained in that study at a flow rate of 1 mL/min (see Fig. 1, Ref. [24]), which was obtained using a PDA detector. Unfortunately, neither the size nor length of tubing used from the outlet of the column to the inlet of the detector was originally specified, but the ID was subsequently confirmed as being 0.005 in. [40]. Hence, their result for band spreading would most closely correspond to our alternate configuration 3, except for the increased size of the post-column tubing, for which we measured a σ^2_{ec} of ~34 μL^2 at 1 mL/min.

A more sophisticated analysis of these results was carried out using Eq. (4) to provide an *estimate* of the relative magnitudes of the individual contributions to ECD for the different configurations studied. The calculated results are presented in Table 4 and again compared to the experimentally measured values obtained for w_{ec}.

As can be seen, the total dispersion for configuration 1 is dominated by the relatively large values contributed by the connective tubing and the detector cell volumes. Whereas, for the other configurations studied, these contributions become progressively smaller, until for alternate configuration 3 they are comparable to the variance contributed by σ^2_{elec}. A best-fit estimate of the additional dispersion observed in the initial experiments, here termed σ^2_{diff}, was calculated for the lowest ECV configurations. That is, the best-fit value for σ^2_{diff} was obtained by incrementing its value until the percent difference values in Table 4 were reduced to approximately equally minimal values for both configuration 3 and alternate configuration 3. A derived value of ~26 μL^2 was obtained for σ^2_{diff}. Note, this is just another way of quantifying the additional dispersion already estimated at ~20–30 μL^2 from the offset observed in the flat section of the curves obtained at lower flow

Table 4
Calculated individual contributions to ECD and derived extra-column volume (w_{ec}) values as a function of instrument modification level and comparison to experimentally measured values. See Table 1 for descriptions of each configuration. All calculated values were derived using Eq. (4), with the following parameters: F = 1 mL/min, F' = 0.32 mL/min, $K_{inj} = K_{cell} = 3$, τ = 0.1 s, $D_m = 1.32 \times 10^{-5}$ cm^2/s (value for anisole in 50:50 acetonitrile water at 30 °C [37]), V_{inj} = 2 μL. For values of r, l, V_{cell} see Table 1. Calculated w_{ec} values were obtained from 5 × calc σ_{ec}. Measured w_{ec} values were obtained at a flow rate of 1 mL/min using the no-column method with uracil as the test probe. A best-fit estimate for σ^2_{diff}, the experimentally observed extra dispersion, was calculated such that the discrepancy between the calculated and measured values for σ^2_{ec} was reduced to approximately zero for the lowest ECV configurations. Note that, as the injection module is *common* to all four configurations, then σ^2_{diff} is the same for all four configurations.

Dispersion or band spreading	Calculated dispersion (μL^2)			
	Config. 1	Config. 2	Config. 3	Alt. config. 3
σ^2_{inj}	1.0	1.0	1.0	1.0
σ^2_{conn}	54.8	17.4	5.2	2.3
σ^2_{det}	25.0	1.7	1.7	0.7
σ^2_{elec}	2.8	2.8	2.8	2.8
σ^2_{diff}	26	26	26	26
Total σ^2_{ec}	109.6	49	37	33
Calc. w_{ec} (μL)	52.3	35.0	30.3	28.6
Meas. w_{ec} (μL)	56	33	30	29
Meas. – Calc. w_{ec}	3.7	−2.0	−0.3	0.4
% difference	6.5%	−6.0%	−1.0%	1.3%

rates in Fig. 1(b)–(d). Again, this value is only an estimate of σ^2_{diff}, as the absolute value is dependent on the way w_{ec} is measured (see above). When this amount of additional dispersion was incorporated into the calculations for the other configurations studied, the discrepancies between the calculated and measured values of σ^2_{ec} in each case were also largely resolved. That is, despite the inherent assumptions in Eq. (4), the experimentally derived results and calculated results are in reasonable agreement (≤7% relative deviation) for all three configurations. The results of additional experiments to determine the origin of σ^2_{diff} are presented in the following sections.

4.3. van Deemter measurements with autosampler injection

The influence of mobile phase linear velocity on plate height was examined in more detail by generating van Deemter plots for the different instrument configurations. Many investigators have published van Deemter measurements using 2.7 μm Fused-Core® columns, see for example [6,13,10]. In those studies, the typical minimum reduced plate height that has been reported for low molecular weight compounds is ~1.5, which corresponds to minimum HETP values of ~4 μm. Van Deemter plots for Fused-Core® columns are also characterized by the relatively small increase in plate height when the mobile phase velocity is increased above the optimum, typically up to 7 mm/s. For our investigations anisole and ethylbenzene were used as test probes and the resulting van Deemter plots are shown in Fig. 2. Note that the plate counts have *not* been corrected for extra-column effects in order to show the observed column efficiencies with the different system configurations.

Anisole was selected as an example test probe for these experiments, because it would be significantly affected by extracolumn dispersion at its relatively low retention factor of 2.2 under the prescribed conditions. Ethylbenzene was chosen for comparison as it has a much higher k value than anisole, so the plate height measurements with this compound would be less influenced by the amount of ECV present in the system. These plots show the expected progressive improvement in column efficiency (N_{obs}) for configurations 1–3 as the ECV is reduced. This improvement is clearly more pronounced for anisole (k = 2.2) than for ethylbenzene

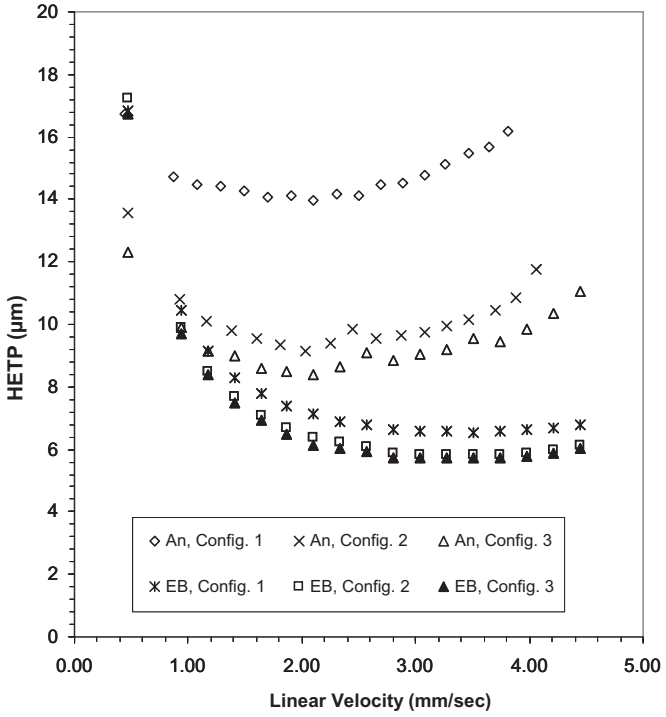

Fig. 2. van Deemter measurements for configurations 1–3. Anisole (k = 2.2) and ethylbenzene (k = 7.2) were used as test probes. Column: HALO® C_{18} 3 mm ID × 100 mm. Note: plate counts have not been corrected for extra-column effects in order to show differences between configurations. The theoretical minimum HETPs at k = 2.2 and k = 7.2, calculated with 32 μL of extra-column band broadening (w_{ec}) in each case, are 8.4 μm and 4.8 μm respectively (see text). Abbreviations for data legend: An, anisole; EB: ethylbenzene.

(k = 7.2), as would be expected from theory. Uncorrected minimum plate heights of 8.5 μm and 5.7 μm were obtained from the anisole and ethylbenzene plots, respectively. At these k values the theoretical minimum HETP values for anisole and ethylbenzene for configuration 3 (w_{ec} = 32 μL, see Table 3), are 8.7 μm and 4.8 μm, respectively. (These latter values were calculated using the expression $\text{HETP} = 10^4 \times L/N_{obs} = 10^4 \times L/[1/N_{col} + w^2_{ec}/16V^2_{col}(1+k)^2]$, which can be derived from Eq. (5), where N_{col} = 24,700, V_{col} = 356 μL and L = 10 cm). The measured and calculated minimum HETP values are in good agreement for anisole, but not for ethylbenzene, where the observed dispersion is greater than predicted. This will be discussed further in the next section.

4.4. Determination of extra-column dispersion using manual valve injection

The origin of the discrepancy between the measured ECD values and those calculated from Eq. (4) (σ^2_{diff} in Table 4) was further investigated by repeating the no-column measurements for configuration 3 and alternate configuration 3 in manual injection mode. This was accomplished by using a low-dispersion injection valve in place of the Alliance 2695 auto-injector. The manual valve was connected in such a way that the estimated minimum ECV (from injection valve to detector) for each injection mode were very similar (see Section 3.2 and Table 1). The ECD results obtained with manual injection are shown in Fig. 3(a) and (b) using both uracil and naphtho[2,3-a]pyrene as test probes, together with the corresponding theoretical results generated from Eq. (4) for comparison.

The following observations can be made. Firstly, for the flow rate range examined, the ECD values for manual injection are significantly lower than values obtained with auto-injection and are reasonably independent of flow rate. Note that, as the peak width

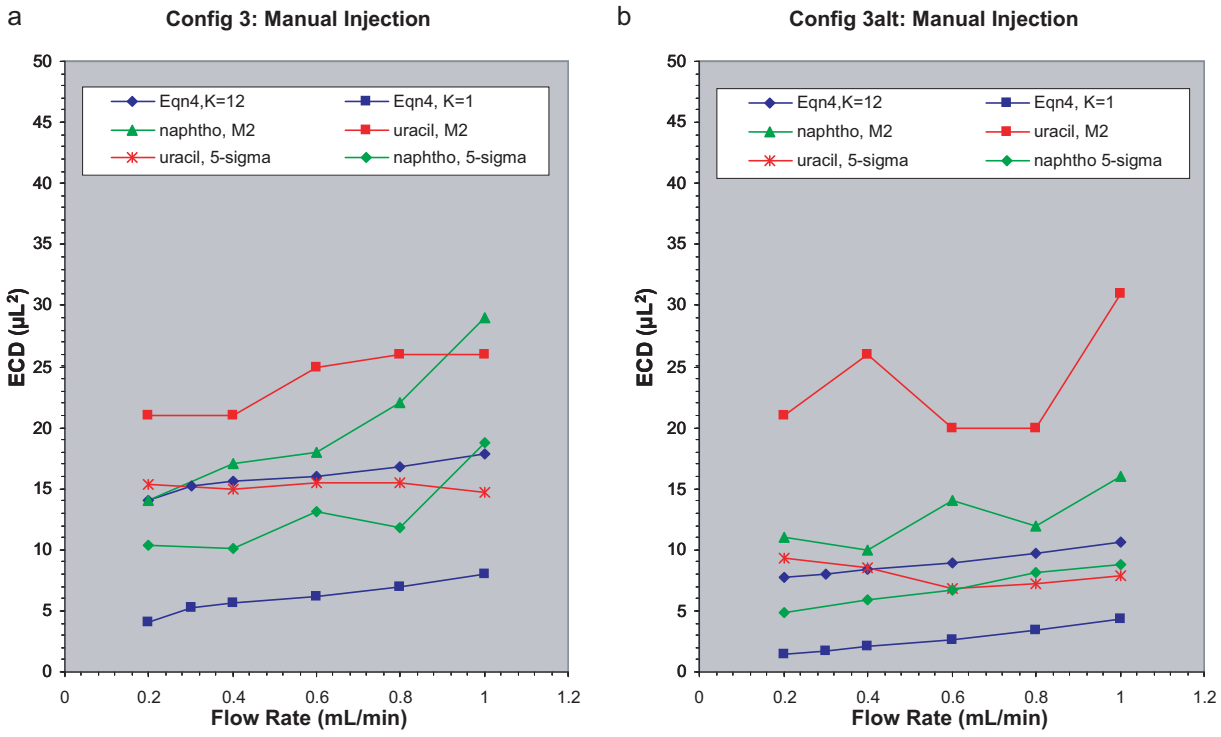

Fig. 3. (a and b) Measured ECD (σ^2_{ec}) values as a function of flow rate for configurations 3 and 3alt using manual injection: (a) configuration 3 and (b) alternate configuration 3. The test analytes were uracil with mobile phase 50/50 (v/v) acetonitrile:water and naphtho[2,3-a]pyrene with mobile phase 100% acetonitrile in each case. For each analyte, both the second moment (M_2) and 5σ-derived dispersions are shown. The theoretical peak variances as a function of flow rate, obtained from Eq. (4) are also plotted with the following limits for the constants: $1 < K_{inj} < 12$ and $1 < K_{cell} < 12$.

in manual injection mode was so much narrower, measurements could only be made up to a maximum flow rate of 1 mL/min without significantly broadening the peak due to the time constant and sampling rate limitations of the detectors (see Sections 2.4 and 2.5). Secondly, for configuration 3, the measured ECV ($w_{ec} \sim 19$ µL) and the estimated ECV (14.5 µL, see Section 3.2) are in better agreement when manual injection is employed. Thirdly, ECD values in manual mode are lowest for alternate configuration 3, which has the lowest estimated ECV (7.5 µL, see Section 3.2).

For configuration 3 and alternate configuration 3, Eq. (4) predicts the correct trend of the experimentally observed dispersion as a function of flow rate up to the maximum flow studied. The absolute values of the experimental and calculated dispersions are now in much closer agreement, and the degree of offset, previously observed with auto-injection, has now been substantially reduced. Indeed, the 5-sigma generated data lies between the two boundary conditions represented by $1 < K_{inj} < 12$ and $1 < K_{cell} < 12$, whereas the M_2 variance data is only off-set by a maximum of ~5 µL^2. Thus, under these conditions, Eq. (4) would appear to provide some useful guidance on the magnitudes of the various contributions to the extra column dispersion, and to predict correctly the increase in total dispersion with increasing flow rate. The one caveat being that, due to the restrictions inherent with the detector employed in this study, it was not possible to test this conclusion at higher flow rates. However, other researchers [14,15], with low dispersion instruments employing fast detectors, have produced similar relatively flat plots of extra column dispersion with increasing flow rate up to 2 mL/min.

The peak profiles obtained at 1 mL/min with manual injection are shown in Fig. 4 together with those previously obtained with auto-injection for comparison purposes. The difference in peak width between configuration 1 with auto-injection and alternate configuration 3 with manual injection is striking. These results clearly confirm that the Alliance 2695 auto-injector module itself

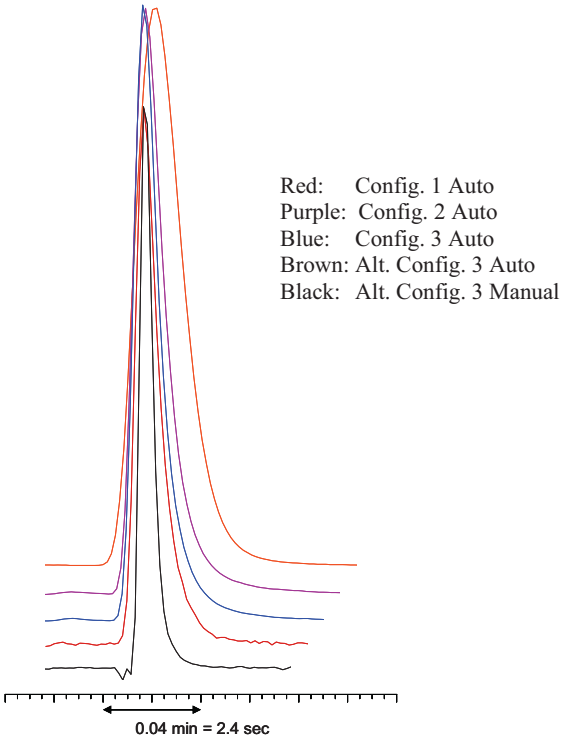

Fig. 4. Influence of extra column band dispersion on peak profiles obtained using the no-column method to determine w_{ec}. Test probe: naphtho[2,3-a]pyrene, flow rate: 1 mL/min, mobile phase: 100% acetonitrile, and injection volume: 1 µL. The colors of the traces from top to bottom are red, purple, blue, brown and black respectively. (For interpretation of the references to color in this figure legend, the reader is referred to the web version of the article.)

is a significant source of extra-column dispersion; unfortunately, this is the one part of the system that cannot be easily modified by the end user.

As shown in Fig. 3(a) and (b), with manual injections, a significant decrease in ECD was obtained. If the Alliance system is examined conceptually, with and without the auto-injector in the *sample flow path*, the following equation may be constructed:

$$\sigma^2_{ec,auto} = \sigma^2_{ec,man} + \sigma^2_{diff}$$

where $\sigma^2_{ec,auto}$ is the total ECD in μL^2 for the 2695 system with auto-injector in the sample flow path, $\sigma^2_{ec,auto}$ is the ECD in μL^2 for manual injections (auto-injector not in sample flow path), and σ^2_{diff} is the difference in peak variance between the two, which is attributed to the dispersion caused by the auto-injector itself. Referring again to Fig. 3 (configuration 3), the extra-column volume with manual injections, $w_{ec,man}$, where $w_{ec,man} = 5 \times \sigma_{ec,man}$, was consistently ~19 μL (average of both uracil and naphtho[2,3-a]pyrene measurements). This value is much smaller than that obtained for auto-injections, $w_{ec,auto}$, where $w_{ec,auto} = 5 \times \sigma_{ec,auto}$, which was ~31.5 μL (Table 3, configuration 3, average of both uracil and naphtho[2,3-a]pyrene measurements at 1 mL/min). This lower value of ~19 μL is consistent with the removal of ~26 μL^2 of ECD (σ^2_{diff}) from the Alliance 2695 (see Table 4) by removing the auto-injector from the sample path and replacing it with a manual injector. That is, from the above equation, the predicted value for $w_{ec,man}$ is:

$$w_{ec,man} = 5 \times \left[\left(\frac{w_{ec,auto}}{5} \right)^2 - \sigma^2_{diff} \right]^{1/2}$$

That is, $w_{ec,manual} = 5 \times [(31.5\ \mu L/5)^2 - 26\ \mu L^2]^{1/2} = 18.5\ \mu L$.

Thus, for manual injections, the measured (~19 μL) and predicted (~18.5 μL) extra-column volumes are in good agreement.

4.5. Determination of column efficiencies using configuration 3

Having modified the Alliance 2695 to reduce the ECD to a minimum, the expected increase in column performance was evaluated using a range of HALO® C_{18} column geometries (3.0 mm ID × 100 mm, 4.6 mm ID × 50 mm, and 2.1 mm ID × 50 mm). The sample was a test mixture of substituted benzenes and the separations were performed isocratically. Typical chromatograms, obtained with auto-injector versus manual injection, are shown in Fig. 5 for the 3.0 mm ID × 100 mm column. Note the significant reduction in peak width and tailing obtained for the early eluting components with manual injection. The measured column efficiencies (N_{obs}) obtained for selected components are shown in Table 5 as a function of injection mode and are compared to the expected plate count (N_{col}). For comparison, the following information is also included in Table 5: (1) the actual w_{ec} values measured for configuration 3 obtained using the no-column method, and (2) the calculated maximum allowable w_{ec} values required to maintain ≥ 90% R_s/81% plates for benzonitrile, 1-chloro-4-nitrobenzene and toluene, respectively.

The theoretical maximum w_{ec} values shown in Table 5 have been calculated in order to maintain ≥90% R_s/81% plates. Therefore, when the measured w_{ec} is less than, or equal, to the predicted w_{ec} (for a given column and k value), good agreement with theory will be indicated if the obtained N_{obs} values are close to 81% of N_{col}. Considering first the results obtained with the 4.6 mm ID column, the predicted w_{ec} values are 20.3 and 37.1 μL for $k = 1.3$ and 3.2 respectively, and the measured w_{ec} values for manual and auto-injections are ~20 and ~36 μL respectively. Therefore, one would expect the measured N_{obs} values to be closer to theoretical at $k = 1.3$ for manual injection and $k = 3.2$ for auto-injection, which is indeed

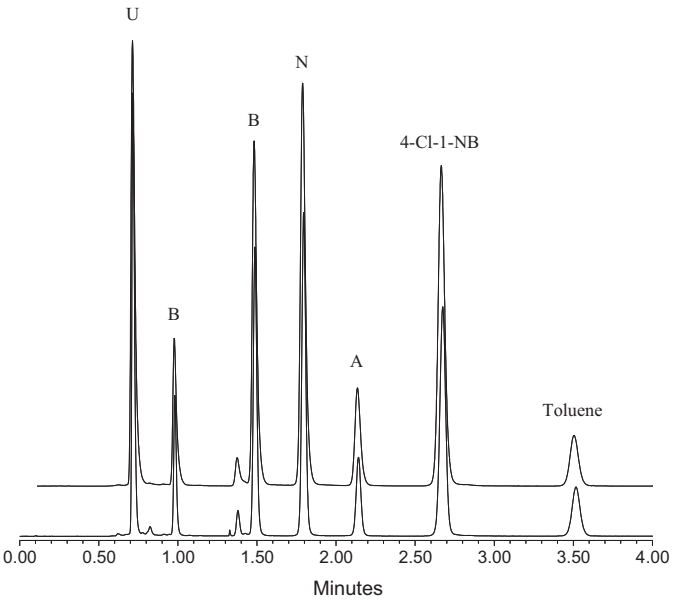

Fig. 5. Chromatograms of seven component test mixture obtained using configuration 3 with a HALO® C_{18} 3 mm ID × 100 mm column. Upper trace: auto-injection and lower trace: manual injection. A flow rate of 0.64 mL/min and an injection volume of 2 μL were used in each case. Abbreviations: A, anisole; BA, benzyl alcohol; BN, benzonitrile; NB, nitrobenzene; 4-Cl-1-NB, 1-chloro-4-nitrobenzene; U, uracil.

the case (76% for $k = 1.3$ and 70% for $k = 3.2$ respectively). For the 3 mm ID column, the experimental w_{ec} value for manual injection (~19 μL) is slightly less that the theoretical value of 23 μL calculated for $k = 3.2$. Therefore, N_{obs} would be expected to be close to the theoretical value, and indeed the measured value is 82%. Whereas, the measured w_{ec} value with the same column using auto-injection is ~30 μL, which is greater that both of the predicted maximum w_{ec} values (12.6 or 23 μL in Table 5), and hence it would be expected that N_{obs} would be significantly smaller than 81% of N_{col}, which was confirmed experimentally. Note that a 2.1 mm ID × 50 mm HALO® Fused-Core® column was also included in this study for the sake of completeness. This column size was not expected to be a practical geometry for isocratic separations on a conventional HPLC system such as the Alliance, as equation 5 predicts a maximum acceptable w_{ec} of only 8.2 μL to maintain ≥90% R_s/81% plates, even for a k value of 3.2. The results in Table 5 confirm this expectation.

In summary, manual injections allowed close to theoretically achievable plate counts (81% of N_{col}) to be obtained using both

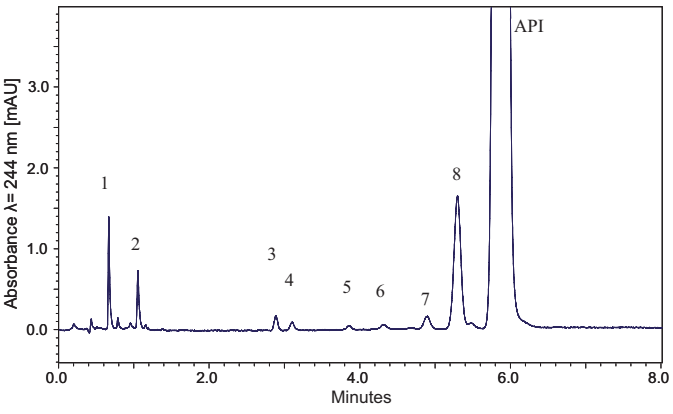

Fig. 6. Chromatogram of pharmaceutical BMS-708163 obtained with configuration 3 using a HALO® C_{18} 3 mm ID × 100 mm column. Early eluting low-level components are numbered 1–8. Note: the remainder of the chromatogram for the end of the gradient program is not shown.

Table 5
Measured column efficiency (N_{obs}) as a function of injection mode for configuration 3 for selected k values. The values in square brackets are the N_{obs} values expressed as a percentage of N_{col} in each case. Measurements were obtained at a constant optimum linear velocity of 3 mm/s with HALO® C_{18} columns having different diameters. See Section 3 for descriptions of the configuration for each injection mode. The peak at k = 1.3 is benzonitrile, the peak at k = 3.2 is 1-chloro-4-nitrobenzene and the peak at k = 4.5 is toluene. The values for N_{obs} are average values, calculated at 5σ peak width, from two replicate injections.

Column size (mm)	Flow rate (mL/min)	N_{col} (theor.)	Inj. mode	N_{obs} (k 1.3)	N_{obs} (k 3.2)	N_{obs} (k 4.5)	Meas. w_{ec} (μL) [No-Col.][b]	w_{ec} (μL) for 90% R_s at k 1.3[a]	w_{ec} (μL) for 90% R_s at k 3.2[a]
4.6 × 50	1.5	~13,200	Manual	10,018 [76%]	11,592 [88%]	11,649 [88%]	~20	20.3	37.1
			Auto	5,775 [44%]	9,278 [70%]	10,370 [79%]	~36		
3 × 100	0.64	~24,700	Manual	16,669 [67%]	20,370 [82%]	20,153 [82%]	~19	12.6	23.0
			Auto	7526 [30%]	14,130 [57%]	16,648 [67%]	~30		
2.1 × 50	0.32	~11,600	Manual	2,490 [21%]	5,575 [48%]	6,904 [60%]	~19	4.5	8.2
			Auto	935 [8%]	2,777 [24%]	4,015 [35%]	~30		

[a] Calculated maximum allowable w_{ec} value (from Eq. (5)) at selected k value, in order to maintain over 90% of the resolving power (R_s), which corresponds to N_{obs}/N_{col} = 0.81. Theoretical N_{col} values were calculated assuming reduced plate heights for 4.6, 3, and 2.1 mm ID columns of 1.4, 1.5, and 1.6, respectively. Note: these reduced plate heights were assigned based on actual average plate counts from column production.
[b] Measured at 5σ peak width using no-column method at respective flow rate with uracil as the test probe.

3 mm ID and 4.6 mm ID columns for $k \geq \sim 3$, when operated at the optimum linear velocity (3 mm/s). On the other hand, even for solutes with $k \geq \sim 4.5$, only ~67–79% of N_{col} was obtained for the same columns in auto-injection mode. Moreover, all peaks were more symmetrical with manual injections. That is, asymmetry factors ranging from 2.03 for uracil to 1.10 for toluene (data obtained in auto-injection mode) were reduced to 1.72 and 1.02, respectively, with manual injection (data not shown). Note, in the case of a more "real-world" flow rate, the column efficiency will be reduced somewhat from the values shown in Table 5. For example, with ethylbenzene as the test probe (k = 7.2), N_{obs} values, measured at 4σ, were found to decrease from 17,467 at 0.65 mL/min to 16,621 at 0.95 mL/min (see van Deemter plots in Fig. 2). These results further confirm that the Alliance 2695 auto-injector module itself is a significant source of extra-column dispersion.

4.6. Impurity profiling of BMS-708163 and BMS-727740

Gradient elution is generally used for the impurity profiling of pharmaceutical compounds because potential impurities can span a wide range of polarities. In gradient mode, extra-column effects also influence chromatographic performance [43]. However, because apparent gradient retention factors (k^*) are approximately constant for different compounds in a linear-gradient separation [44], each peak in the chromatogram is affected similarly by extra-column dispersion contributions. Pre-column band spreading is often minimal, because starting mobile phase conditions are chosen so that most analytes are strongly retained at the start of the gradient, and are therefore "focused" at the column inlet [45]. Conversely, post-column band spreading can still be significant, and will be greatest for the narrowest peaks (highest efficiency, lowest volume columns, and steepest gradients). High peak capacity separations of peptides on columns packed with Kinetex™-C_{18} [46] and HALO® C_{18} [47,48] porous shell particles have been reported in gradient elution chromatography. In the two examples given below, each separation was obtained using a 7-min isocratic segment as the start of the separation method followed by a rapid gradient to 100%B. Thus, any impurities with retention times shorter than that of the API (active pharmaceutical ingredient) are eluted under isocratic conditions. Such isocratic conditions, under which the less retained impurities followed by the API elute, represent "worst case scenarios" for assessing the impact of extra-column dispersion on observed efficiencies and peak shapes.

The impurity profile of BMS-708163 obtained using a 3 mm ID × 100 mm HALO C_{18} column at 0.9 mL/min is shown in Fig. 6. Impurities 1–8 elute under isocratic conditions, and are, therefore, useful markers to assess real-world instrument performance with respect to ECV and ECD. The efficiency and resolution data for selected early-eluting components (impurities 1–4), which are affected most by reduction in ECV, are shown in Table 6 for configurations 1 and 3.

Both column efficiency and resolution show the expected improvements for data obtained using lower ECV configuration 3. In addition, even with the smaller flow cell used with configuration 3, very low level impurities can still be detected with satisfactory signal-to-noise (S/N) ratios so that LOQs (limits of quantitation, S/N > 10) can be obtained at the required 0.05% (w/w) level. Note that the N_{obs} values shown in Table 6 are lower than those obtained using the seven-component test mixture (see comparable values in Table 5 for k = 1.3 and auto-injection). This is most likely due to a number of small experimental differences, which are known to cause increased sample dispersion. That is, in the case of BMS-708163, the sample solvent was somewhat stronger than the initial mobile phase and the injection volume was larger (3 μL versus 2 μL). In addition, the column temperature was 10 °C higher, and as no heater exchanger was used in order to minimize the pre-column ECV, this may have introduced extra dispersion due to a possible thermal mismatch between the column temperature and the entering mobile phase temperature.

In Fig. 7, an expanded portion of the impurity profile of BMS-727740 is shown. The upper and lower traces were obtained using configurations 1 and 3, respectively, and show impurities C and D which elute just before and just after the API, respectively. These impurities are present at 1.77 and 1.16 area percent, respectively. The chromatogram obtained using configuration 3 shows a significant improvement in resolution over the one obtained using

Table 6
Efficiency (N) and resolution (R_s) results for selected early eluting components in chromatograms of pharmaceutical drug substance BMS-708163 (shown in Fig. 7) as a function of Alliance 2695 configuration. Config. 1, 56 μL measured ECV; config. 3, 30 μL measured ECV (see w_{ec} values obtained with uracil in Table 3).

Instrument config.	Efficiency (N_{obs})				Resolution (R_s)	
	Peak 1 k = 0.6, area% 0.22, S/N 158	Peak 2 k = 1.6, area% 0.14, S/N 80	Peak 3 k = 6, area% 0.07, S/N 20	Peak 4 k = 6.7, area% 0.04, S/N 10	Peaks (1 and 2)	Peaks (3 and 4)
Config. 1	2,187	4,120	14,174	12,793	6.1	1.8
Config. 3	3,845	5,503	14,251	11,209	8.8	2.1

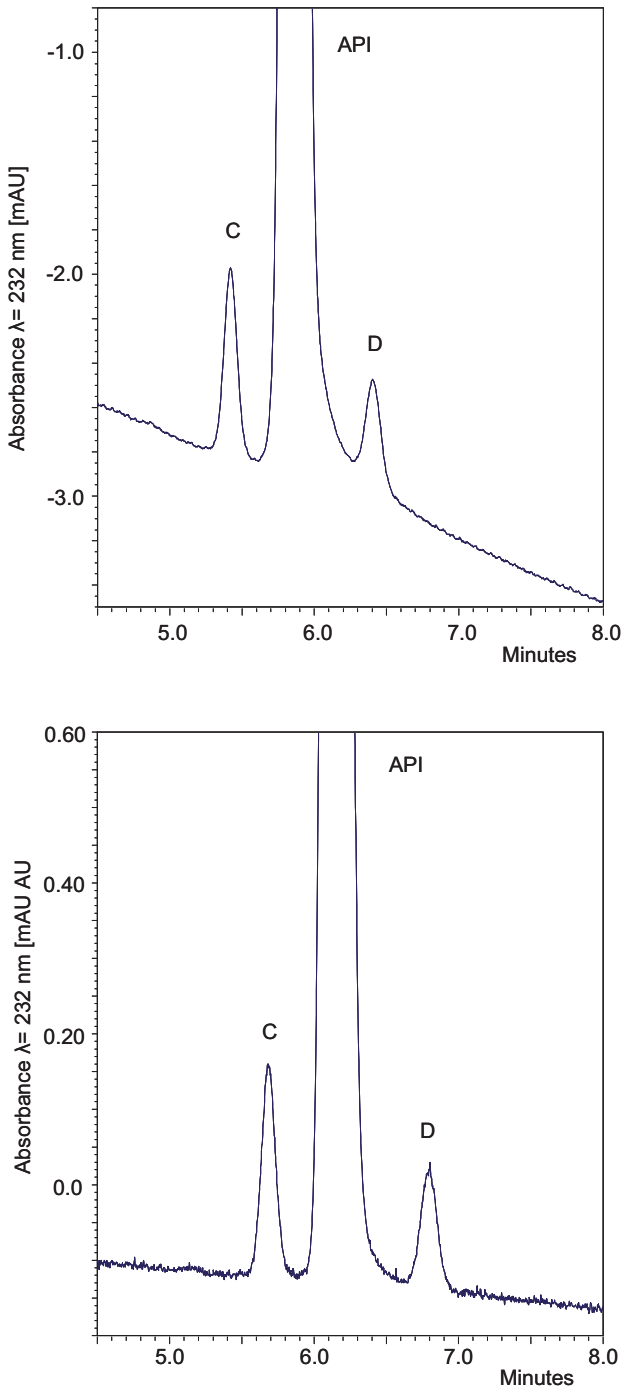

Fig. 7. Expanded section of chromatogram of pharmaceutical BMS-727740 showing impurities eluting close to that of the retention time of the API. The upper and lower traces were obtained with configurations 1 and 3, respectively using a HALO® C_{18} 3 mm ID × 100 mm column. Note: the absorbance scales for upper and lower traces are different.

configuration 1, while the S/N ratios (27 for impurity C and 15 for impurity D) are more than adequate for low-level quantitation. Actual resolution values obtained between the API and impurity D were 2.52 for configuration 1 and 3.12 for configuration 3. It is of note that the original run times for these two methods, employing traditional 4.6 mm ID × 150 mm, 3.0 μm columns, were 40 min for BMS-708163 and 45 min for BMS-727740. These run times were reduced to just 13 min in each case by appropriate scaling of the methods to employ 3.0 mm ID × 100 mm, 2.7 μm Fused-Core® columns.

5. Conclusion

In this case study, we have examined the impact of ECD from a Waters Alliance 2695 on the performance of 2.7 μm Fused-Core® columns of various dimensions. The system was re-configured in different ways to reduce ECV and the resulting ECD measured as a function of flow rate. The results obtained showed a progressive decrease in ECD from configuration 1 to alternate configuration 3, which is consistent with the concomitant decrease in ECV.

However, this decrease in ECD, to a minimum of ~34 μL^2 at 1 mL/min for the lowest ECV configuration, was less than theoretically expected at that flow rate. The inability to reduce the actual extra-column dispersion further was attributed to ~26 μL^2 of additional dispersion associated with the design/volume of the auto-injector. This is a fixed amount of dispersion, and hence becomes a progressively larger percentage of the total dispersion as the ECV of the system is reduced. Unfortunately, this limits the improvement that can be obtained by just reducing the dispersion contributions from other sources. This was confirmed by making sample injections with a low dispersion manual injection valve, instead of auto-injection. For example, in the case of configuration 3 with manual injection, the ECD was reduced to ~15 μL^2. This result was derived from the measured w_{ec} value of ~19 μL, a value that is now in reasonable agreement with that of the estimated ECV (~14.5 μL). The auto-injector module is an integral part of the Alliance 2695 instrument and cannot be easily modified. However, even with autosampler injection, for a 3 mm ID × 100 mm Fused-Core® column approximately 70% of the maximum plate count (~84% of the resolution or more) could still be obtained in isocratic separations for solutes with $k \geq \sim 4.5$ when using the lowest ECV configuration. The theoretically expected dispersion was also modeled using Eq. (4) with the boundary conditions $1 < K_{inj} < 12$ and $1 < K_{cell} < 12$. The results were found to be practically useful and gave the best agreement with experiment for the lowest ECV configurations studied in conjunction with manual injection. However, it must be stressed that Eq. (4) is an idealized model of the contributions to extra column dispersion and it was not possible to test rigorously its applicability over a wide flow rate range.

Using a modified Alliance 2695 instrument with the aforementioned column geometry, we have demonstrated the conversion of two real-world pharmaceutical impurity method separations to improved separations that are ~3–3.5 times faster, while maintaining data quality in terms of resolution and signal-to-noise ratio. Significant improvements in resolution and theoretical plates, particularly for early eluting components ($k \leq \sim 5$), were achieved after making modifications of the instrument to reduce ECV. These two examples were selected because the original impurity methods had initial isocratic conditions followed by linear gradients to elute the more highly retained impurities and to prepare the column for subsequent runs. Such isocratic conditions, under which the less retained impurities, followed by the API, elute, represent "worst case scenarios" for assessing the impact of extra-column dispersion on observed efficiencies and peak shapes. We would expect that 3 mm ID Fused-Core® columns even shorter than 100 mm would perform well using a modified Alliance system in a linear, or segmented gradient, without much impact from extra-column volume, because of on-column focusing and gradient band compression. However, the observed efficiencies of shorter columns may not be high enough to provide the necessary resolution for impurity profiling of complex samples. Gradient separations are, however, still influenced by post-column tubing volume, flow cell volume, data sampling rate, and detector time constant, and conventional HPLC systems must be modified and analysis conditions set so that desired or acceptable performance can be obtained with low-volume, high efficiency columns.

References

[1] R.E. Majors, LC–GC 28 (2010) 8.
[2] E. Van Gyseghem, M. Jimidar, R. Sneyers, M. De Smet, E. Verhoeven, Y. Vander Heyden, J. Pharm. Biomed. Anal. 41 (2006) 751.
[3] J. Ringling, C. Wood, R. Borjas, C. Foti, Am. Pharm. Rev. 11 (2008) 24.
[4] M.W. Dong, LC–GC 25 (2007) 656.
[5] N. Wu, A. Clausen, L. Wright, K. Vogal, F. Bernardoni, Am. Pharm. Rev. 11 (2008) 24.
[6] J.J. Kirland, T.J. Langlois, J.J. DeStefano, Am. Lab. 39 (2007) 18.
[7] http://www.phenomenex.com/Phen/EM/ws63990808/technology.html.
[8] S. Fekete, J. Fekete, K. Ganzler, J. Pharm. Biomed. Anal. 49 (2009) 64.
[9] F. Gritti, I. Leonardis, D. Shock, P. Stevenson, A. Shalliker, G. Guiochon, J. Chromatogr. A 1217 (2010) 2589.
[10] F. Gritti, A. Cavazzini, N. Marchetti, G. Guiochon, J. Chromatogr. A 1157 (2007) 289.
[11] A. Cavazzini, F. Gritti, K. Kaczmarski, N. Marchetti, G. Guiochon, Anal. Chem. 79 (2007) 5972.
[12] A. Abrahim, M. Al-Sayah, P. Skrdla, Y. Bereznitski, Y. Chen, N. Wu, J. Pharm. Biomed. Anal. 51 (2010) 131.
[13] J.J. DeStefano, T.J. Langlois, J.J. Kirland, J. Chromatogr. Sci. 46 (2008) 254.
[14] D.V. McCalley, J. Chromatogr. A 1217 (2010) 4561.
[15] F. Gritti, C.A. Sanchez, T. Farkas, G. Guiochon, J. Chromatogr. A 1217 (2010) 3000.
[16] "Modifying Agilent 1100 HPLC System to Achieve UPLC-Like Performance with HALO Fused-Core Columns", Tech. Report LC501, MAC-MOD Analytical, Inc., Chadds Ford, PA, 2008, 6 pp.
[17] T.L. Chester, Am. Lab. 41 (2009) 11.
[18] J.C. Sternberg, in: J.C. Giddings, R.A. Kelly (Eds.), Advances in Chromatography, Marcel Dekker, New York, 1966.
[19] G. Guiochon, in: J.C. Giddings, C. Horvath (Eds.), High-Performance Liquid Chromatography, Advances and Perspectives, vol. 2, Academic Press, Inc., New York, 1980.
[20] R.P.W. Scott, J. Liq. Chromatogr. Related Technol. 25 (2002) 2567.
[21] V.L. McGuffin, in: E. Heftmann (Ed.), Chromatography, Part A: Fundamentals and Techniques, J. Chromatogr. Lib., vol. 69A, 6th edn, Elsevier, Amsterdam, 2004, p. 33.
[22] J.C. Gluckman, M. Novotny, in: M.V. Novotny, D. Ishii (Eds.), Microcolumn Separations, J. Chromatogr. Lib., vol. 30, Elsevier, New York, 1985, p. 57.
[23] R. Russo, D. Guillarme, D.T.-T. Nguyen, C. Bicchi, S. Rudaz, J.-L. Veuthey, J. Chromatogr. Sci. 46 (2008) 199.
[24] K.J. Fountain, U.D. Neue, E.S. Grumbach, D.M. Diehl, J. Chromatogr. A 1216 (2009) 5979.
[25] Waters 2690 Separations Module Operator's Guide, Waters Corporation, Milford, 1996, p. 1.
[26] R.P.W. Scott, Liquid Chromatography Detectors, J. Chromatogr. Lib., vol. 33, Elsevier, New York, 1986, p. 36.
[27] D. Guillarme, D.T.-T. Nguyen, S. Rudaz, J.-L. Veuthey, Eur. J. Pharm. Biopharm. 66 (2007) 475.
[28] A. Prüß, C. Kempter, J. Gysler, T. Jira, J. Chromatogr. A 1016 (2003) 129.
[29] M.W. Dong, in: S. Ahuja, M.W. Dong (Eds.), Handbook of Pharmaceutical Analysis by HPLC, Separation Science and Technology, vol. 6, Elsevier, San Diego, CA, 2005, p. 69.
[30] F. Gritti, G. Guiochon, J. Chromatogr. A 1166 (2007) 30.
[31] J.M. Miller, Chromatography: Concepts and Contrasts, 2nd edn, Wiley Interscience, Hobroken, NJ, 2005, p. 287.
[32] L.R. Snyder, J.J. Kirkland, J.W. Dolan, Introduction to Modern Liquid Chromatography, 3rd edn, John Wiley and Sons Ltd., Hobroken, NJ, 2010, p. 502.
[33] K.W. Gillman, J.E. Starrett Jr., M.F. Parker, K. Xie, J.J. Bronson, L.R. Marcin, K.E. McElhone, C.P. Bergstrom, R.A. Mate, R. Williams, J.E. Meredith Jr., C.R. Burton, D.M. Barten, J.H. Toyn, S.B. Robetrs, K.A. Lentz, J.G. Houston, R. Zaczek, C.F. Albright, C.P. Decicco, J.E. Macor, R.E. Olsen, ACS Med. Chem. Lett. 1 (2010) 120.
[34] US patent application publication US2005/0267105 published December 1, 2005, The compound is shown as example 82 and in Claim 15.
[35] H.H. Lauer, G.P. Rozing, Chromatographia 14 (1981) 641.
[36] H.A. Claessens, C.A. Cramers, M.A.J. Kuyken, Chromatographia 23 (1987) 189.
[37] "How to Measure and Reduce HPLC Equipment Extra Column Volume", Tech. Report LC507, MAC-MOD Analytical, Inc., Chadds Ford, PA, 2009, 6 pp.
[38] J. Li, P.W. Carr, Anal. Chem. 69 (1997) 2530.
[39] F. Gerber, M. Krummen, H. Potgeter, A. Roth, C. Siffrin, C. Spoendlin, J. Chromatogr. A 1036 (2004) 127.
[40] Personal communication with K.J. Fountain, Waters Corporation, December 9, 2009.
[41] J.J. Baeza-Baeza, S. Pous-Torres, J.R. Torres-Lapasio, M.C. Garcia-Alvarez-Coque, J. Chromatogr. A 1217 (2010) 2147.
[42] F. Gritti, A. Felinger, G. Guiochon, J. Chromatogr. A 1136 (2006) 57.
[43] P. Jandera, J. Churáček, Gradient Elution in Liquid Chromatography: Theory and Practice, J. Chromatogr. Lib., vol. 31, Elsevier, New York, 1985, p. 110.
[44] L.R. Snyder, J.W. Dolan, High Performance Gradient Elution, John Wiley and Sons, Hobroken, NJ, 2006, p. 34.
[45] P. Jandera, J. Churáček, Gradient Elution in Liquid Chromatography: Theory and Practice, J. Chromatogr. Lib., vol. 31, Elsevier, New York, 1985, p. 101.
[46] F. Gritti, G. Guiochon, J. Chromatogr. A 1217 (2010) 1604.
[47] N. Marchetti, G. Guiochon, J. Chromatogr. A 1176 (2007) 206.
[48] N. Marchetti, A. Cavazzini, F. Gritti, G. Guiochon, J. Chromatogr. A 1163 (2007) 203.